Available online at www.sciencedirect.com
SCIENCE DIRECT
International Journal of Heat and Fluid Flow 27 (2006) 279–289
International Journal of HEAT AND FLUID FLOW
www.elsevier.com/locate/ijhff

On the prediction of equilibrium states in stably stratified homogeneous sheared turbulence

Ridha Abid [a,*], Ridha Habibi [b]

[a] INSAT, Centre Urbain Nord, B.P. No. 676, 1080 Tunis Cedex, Tunisia
[b] Faculté des Sciences de Tunis, Laboratoire de Mécanique des Fluides, Tunisia

Received 28 February 2002; received in revised form 11 August 2005; accepted 11 August 2005
Available online 14 November 2005

Abstract

An assessment of second-order closure models in the prediction of stratified homogeneous shear flows has been conducted. The emphasis is placed on analyzing the effects of three modeled dissipation rate equations on the prediction of equilibrium states. It is found that second-order closure models are unable to reproduce the main features of stratified homogeneous shear flow. In particular, the models considered cannot predict an important experimental observation, namely, the existence of a stationary gradient Richardson number, Rs, below which the turbulent kinetic energy, K, shows exponential growth and, above which, K, decays exponentially. This result is partly due to deficiencies in the modeled dissipation rate equation.

It is shown, herein, that the performance of second-order closure models will substantially improve if stationary conditions of the turbulent kinetic energy K and the dissipation rate ε are satisfied.

Keywords: Stratification; Homogeneous flow; Turbulent flow; Equilibrium states

1. Introduction

Homogeneous shear flows have served as basic building block flows for screening and calibration of turbulence models since it encapsulates some of the important features of turbulent equilibrium flows.

An initially isotropic turbulence grows after it is subjected to a uniform shear rate S. The turbulent kinetic energy K, the Reynolds stresses $\overline{u_i u_j}$, the dissipation rate ε and the largest length scales grow exponentially in time because the constant shear rate provides an infinite source of turbulent kinetic energy. However, structural equilibrium in the homogeneous shear flow is reached so that the anisotropy Reynolds stress tensor b_{ij} and the shear parameter SK/ε achieve equilibrium values that are independent of the initial conditions. In fact, equilibrium states of several benchmark homogeneous shear flows have been used in the development and analysis of turbulence models (Speziale et al., 1991; Abid and Speziale, 1993).

In recent years, research has been focused on the study of homogenous stably stratified shear flows. Numerous laboratory experiments on vertically stably stratified homogenous shear flows have been performed. Among, the most notable laboratory experiments are those of Rohr et al. (1988) and Piccirillo and Van Atta (1997). On the other hand, numerical simulations of such flows have been carried out by Gerz et al. (1989), Holt et al. (1992), Kaltenbach et al. (1994), Jacobitz (2000, 2002), Jacobitz and Sarkar (1998, 1999), Jacobitz et al. (1997) and Shih et al. (2000).

An initially isotropic turbulence evolves after it is subject to uniform mean shear rate S and uniform stratification (negative mean density gradient S_ρ or positive mean temperature gradient S_T). Hence, the destabilizing effect of mean shear on turbulence (shear supplies turbulent kinetic energy for turbulent motions) competes with the stabilizing effect of stable stratification on turbulence (buoyancy forces act to suppress turbulence). The global

* Corresponding author. Fax: +216 71704 329.
E-mail address: ridha_abid@yahoo.fr (R. Abid).

0142-727X/$ - see front matter © 2005 Elsevier Inc. All rights reserved.
doi:10.1016/j.ijheatfluidflow.2005.08.004

Nomenclature

b_{ij} Reynolds stress anisotropy $= (\overline{u_i u_j}/2K - \delta_{ij}/3)$
$C_1 - C_5$ empirical constants in Eq. (13)
$C_{\theta 1} - C_{\theta 5}$ empirical constants in Eq. (17)
$C_{d1} - C_{d5}$ empirical constants in Eq. (23)
$C_{\varepsilon 1} - C_{\varepsilon 4}$ empirical constants in Eq. (19)
E dimensionless parameter $= (P + G)/\varepsilon$
F_i normalized heat flux $= (g\beta\overline{u_i\theta}/KS)$
F_θ normalized temperature variance $= ((g\beta/S)^2\overline{\theta^2}/K)$
g_i,g gravitational acceleration
G_{ij} buoyant production of $\overline{u_i u_j}$
$G_{i\theta}$ buoyant production of $\overline{u_i\theta}$
G buoyant production of K
K turbulent kinetic energy $= (\overline{u_i u_i}/2)$
L_b buoyancy length scale $= ((\overline{w^2})^{1/2}/N)$
L_E Ellison length scale $= ((\overline{\theta^2})^{1/2}/S_T)$
L_O Ozmidov length scale $= (\varepsilon/N^3)^{1/2}$
N Brunt–Väïsäla frequency $= (g\beta S_T)^{1/2}$
p fluctuating pressure
P turbulence production of $K = (P_{ii}/2)$
P_{ij} shear stress production of $\overline{u_i u_j}$
$P_{i\theta}$ production of $\overline{u_i\theta}$ by mean gradients of U_i and T
P_θ production of $\overline{\theta^2}$
r time scale ratio $= (\overline{\theta^2}\varepsilon/(\varepsilon_\theta K))$
R_f flux Richardson number $= (-G/P)$
Ri gradient Richardson number $= (N^2/S^2)$
Rs stationary gradient Richardson number
R_ε additional term in the dissipation rate equation (Eq. (19))
S mean shear rate $= (\mathrm{d}U/\mathrm{d}z)$
S_T mean temperature gradient $= (\mathrm{d}T/\mathrm{d}z)$
S_{ij} mean rate of strain tensor
t time
T mean temperature
T' instantaneous temperature
T_0 reference mean temperature
u_i fluctuating velocity component in direction x_i
u streamwise velocity fluctuation
U_i mean velocity component in direction x_i
$\overline{u_i u_j}$ Reynolds stress tensor
$\overline{u_i\theta}$ scalar flux tensor
w vertical component fluctuating velocity
w' root mean square of w
u' root mean square of u
W_{ij} mean vorticity tensor
x_i position coordinate
z vertical coordinate

Greeks
α_t Eddy diffusivity
β thermal expansion coefficient $(= 1/T_0)$
γ dimensionless growth rate of $K = ((\mathrm{d}K/\mathrm{d}t)/K)$
δ_{ij} Kronecker delta $= 1$ for $i = j$ and $= 0$ for $i \neq j$
ε dissipation rate of K
ε_{ij} dissipation rate of $\overline{u_i u_j}$
$\varepsilon_{i\theta}$ dissipation rate of $\overline{u_i\theta}$
ε_θ dissipation rate of $\overline{\theta^2}$
η shear parameter $= (SK/\varepsilon)$
$\underline{\theta}$ fluctuating temperature
$\overline{\theta^2}$ temperature variance
θ' root mean square of θ
ν kinematic molecular viscosity
ν_t Eddy viscosity
ϕ_{ij} pressure–strain term of $\overline{u_i u_j}$
$\phi_{i\theta}$ pressure–temperature gradient term of $\overline{u_i\theta}$

Subscript
∞ equilibrium condition

parameter that measures the relative influence of shear and stratification on the flow is the gradient Richardson number $Ri = N^2/S^2$, where N is the Brunt–Väïsälä frequency.

The main findings of these numerical simulations and laboratory experiments of homogeneous stably stratified sheared turbulence can be summarized as follows:

(a) As the gradient Richardson number Ri increases, the total production of the turbulent kinetic energy due to vertical shear (P) and buoyancy forces (G) decreases because the stable stratification acts to reduce turbulence ($G < 0$). Therefore, the dimensionless growth rate γ defined by: $\gamma = \frac{1}{SK}\frac{\mathrm{d}K}{\mathrm{d}t} = \left(\frac{\varepsilon}{SK}\right)(E-1)$ decreases. The parameter $E = (P + G)/\varepsilon$, represents the ratio of the total production of K over the viscous dissipation rate ε.

(b) At a certain value of the Richardson number $Ri = Rs$ (hereafter referred to as the stationary gradient Richardson number), the statistical turbulent quantities (such as the turbulent kinetic energy, dissipation rate and the largest length scales), remain constant in time, a stationary state is reached. Hence, the growth rate γ is zero and $E = 1$. Experimental and DNS results have shown that the turbulent kinetic energy K grows exponentially when $Ri < Rs$ (weak stratification) and decays exponentially when $Ri > Rs$ (strong stratification).

(c) Rohr et al. (1988) carried out experiments on homogeneous turbulence in a stably stratified shear flow in a salt-stratified water-channel. They found that $Rs = 0.25 \pm 0.05$.

Gerz et al. (1989), Holt et al. (1992), Kaltenbach et al. (1994) and Jacobitz et al. (1997) demonstrated the existence of a stationary Richardson number using DNS of sheared stratified flow and found that its value is lower

than 0.25 ($0.04 < Rs < 0.2$) and increases with the Reynolds number.

They suggested that the value of Rs depends on both the Reynolds number and the initial shear parameter of the flow.

Finally, Shih et al. (2000) performed a series of DNS over a range of initial Reynolds numbers and shear parameters. They found that, at lowRe, the value of Rs depend on both Re and (SK/ε), but at higher Re, it varies only with Re; the shear parameter evolves to a constant value (≈ 5.5) regardless of its initial value. Also, the dependence of Re is correlated by the following relationship (Shih et al. (2000)):

$$Rs = 0.25/(1 + 103/Re)$$

Implying that Rs asymptotes to 0.25 for high Re, the value predicted by inviscid linear stability (Miles (1961)).

While incompressible homogeneous shear flows have been studied extensively leading to the development of some reasonable turbulence models, stratified homogeneous shear flows is relatively less scrutinized.

The purpose of the present paper is to study the ability of current second-order closure models to capture the relevant physics of stable stratified homogeneous shear flows using DNS and experimental data. These flows are selected in order to eliminate uncertainties due to numerics and turbulent diffusion modeling. The emphasis of this paper is placed on studying the effects of three modeled dissipation rate equations on the prediction of essential features of these flows.

An attempt also be will made to understand the physical origin of deficient model predictions.

2. Theoretical background

We will consider incompressible, stratified turbulent shear flows governed by the Navier–Stokes, continuity and energy equations subject to the Boussinesq approximation.

The velocity U_i', the pressure P' and the temperature T' are decomposed into standard ensemble mean and fluctuating parts, respectively,

$$U_i' = U_i + u_i, \quad P' = P + p, \quad T' = T + \theta \tag{1}$$

The resulting Reynolds averaged equations contain two unclosed terms, the Reynolds stress tensor $\overline{u_i u_j}$ and the turbulent heat flux $\overline{u_i\theta}$. In this study, turbulence models based on transport equations for the second-order moments $\overline{u_i u_j}, \overline{u_i\theta}, \overline{\theta^2}$ are considered. We will restrict our analysis to vertically stably stratified and vertically homogeneous sheared flow where we have

$$\frac{\partial U_i}{\partial x_j} = S\delta_{i1}\delta_{j3}, \quad \frac{\partial T}{\partial x_j} = S_T\delta_{j3}, \quad g_j = -g\delta_{j3} \tag{2}$$

where S is the constant shear rate, S_T is the constant temperature gradient ($S_T > 0$) and g is the gravitational acceleration.

2.1. Second-order equations

The exact Reynolds stress transport equation is given by

$$\frac{\mathrm{d}}{\mathrm{d}t}\left(\overline{u_i u_j}\right) = P_{ij} + G_{ij} + \phi_{ij} - \varepsilon_{ij} \tag{3}$$

The terms, in the above equation, respectively, are the time rate of change, production due to mean shear (P_{ij}), buoyant production (G_{ij}), pressure strain correlation (ϕ_{ij}) and viscous dissipation rate (ε_{ij}) of Reynolds stress:

$$P_{ij} = -\overline{u_i u_k}\frac{\partial U_j}{\partial x_k} - \overline{u_j u_k}\frac{\partial U_i}{\partial x_k}, \quad \varepsilon_{ij} = 2\nu\overline{\frac{\partial u_i}{\partial x_k}\frac{\partial u_j}{\partial x_k}} \tag{4}$$

$$G_{ij} = -\beta\left(\overline{u_i\theta}g_j + \overline{u_j\theta}g_i\right), \quad \phi_{ij} = \overline{\frac{p}{\rho_0}\left(\frac{\partial u_i}{\partial x_j} + \frac{\partial u_j}{\partial x_i}\right)} \tag{5}$$

given that ν is the kinematic viscosity, ρ_0 is the reference density of the fluid and β is the thermal expansion coefficient. Hence, the production terms are exact but the terms ϕ_{ij} and ε_{ij} require modeling.

If we contract the indices in (3), then we obtain the transport equation for the turbulent kinetic energy, $K = \frac{1}{2}\overline{u_i u_i}$

$$\frac{\mathrm{d}K}{\mathrm{d}t} = P + G - \varepsilon \tag{6}$$

where $P = P_{ii}/2$ is the turbulence production due to mean shear, $G = G_{ii}/2 = -\beta g_i\overline{u_i\theta}$ is production term due to buoyancy forces and $\varepsilon = \varepsilon_{ii}/2$ is the viscous dissipation rate.

The exact equation for the heat flux is

$$\frac{\mathrm{d}}{\mathrm{d}t}\left(\overline{u_i\theta}\right) = P_{i\theta} + G_{i\theta} + \phi_{i\theta} - \varepsilon_{i\theta} \tag{7}$$

The terms, in the above equation, correspond to the time rate of change, thermal production ($P_{i\theta}$), buoyant production ($G_{i\theta}$), pressure–temperature gradient correlation ($\phi_{i\theta}$) and viscous dissipation ($\varepsilon_{i\theta}$):

$$P_{i\theta} = -\overline{u_i u_k}\frac{\partial T}{\partial x_k} - \overline{u_k\theta}\frac{\partial U_i}{\partial x_k}, \quad G_{i\theta} = -\beta g_i\overline{\theta^2} \tag{8}$$

$$\phi_{i\theta} = \overline{\frac{p}{\rho_0}\frac{\partial\theta}{\partial x_i}}, \quad \varepsilon_{i\theta} = (\alpha + \nu)\overline{\frac{\partial\theta}{\partial x_k}\frac{\partial u_i}{\partial x_k}} \tag{9}$$

The only unknown correlation in Eq. (7) for which another transport equation is solved, is the temperature variance $\overline{\theta^2}$. The exact equation for $\overline{\theta^2}$ is

$$\frac{\mathrm{d}}{\mathrm{d}t}\left(\overline{\theta^2}\right) = 2(P_\theta - \varepsilon_\theta) \tag{10}$$

$$P_\theta = -\overline{u_k\theta}\frac{\partial T}{\partial x_k}, \quad \varepsilon_\theta = 2\alpha\overline{\frac{\partial\theta}{\partial x_k}\frac{\partial\theta}{\partial x_k}} \tag{11}$$

In the above equation, the term P_θ is the production of temperature variance and the term ε_θ is the viscous dissipation rate of temperature variance. Hence, exact second-order equations are unclosed. In order to achieve second-order closure, models for ϕ_{ij}, ε_{ij}, $\phi_{i\theta}$ and ε_θ must be provided.

2.2. Second-order closure equations

2.2.1. Models for ϕ_{ij} and $\phi_{i\theta}$

The pressure–strain correlation ϕ_{ij} can be written as a sum of terms corresponding to different sources of the pressure fluctuations (Launder (1996));

$$\phi_{ij} = \phi_{ij,1} + \phi_{ij,2} + \phi_{ij,3} \tag{12}$$

Here, $\phi_{ij,1}$ is the slow term involving product of turbulent fluctuations, $\phi_{ij,2}$ is the rapid term involving the effect of mean strain and $\phi_{ij,3}$ is the buoyancy contribution.

Craft et al. (1996) developed a general model for the pressure–strain and the pressure–temperature gradient correlations consistent with the two-component turbulence limit. This model was successful in predicting several challenging buoyant flows (Craft and Launder (2001)).

For two dimensional unstratified homogeneous flows (simple planar flows), Speziale et al. (1991) have shown that a class of existing models of pressure–strain correlation collapse to the following general form:

$$\begin{aligned}\phi_{ij,1} + \phi_{ij,2} = &-C_1 b_{ij}\varepsilon + C_2 K S_{ij} \\ &+ C_3 K\left(b_{ik}S_{kj} + b_{jk}S_{ki} - \frac{2}{3}b_{mn}S_{mn}\delta_{ij}\right) \\ &+ C_4 K(b_{ik}W_{jk} + b_{jk}W_{ik}) \\ &- C_5\left(G_{ij} - \frac{1}{3}G_{kk}\delta_{ij}\right)\end{aligned} \tag{13}$$

where

$$S_{ij} = \frac{1}{2}\left(\frac{\partial U_i}{\partial x_j} + \frac{\partial U_j}{\partial x_j}\right), \quad W_{ij} = \frac{1}{2}\left(\frac{\partial U_i}{\partial x_j} - \frac{\partial U_j}{\partial x_i}\right),$$
$$b_{ij} = \frac{\overline{u_i u_j}}{2K} - \frac{\delta_{ij}}{3} \tag{14}$$

given that b_{ij} is the Reynolds stress anisotropy tensor, S_{ij} is the mean rate of strain tensor and W_{ij} is the mean vorticity tensor.

In this study, we will use the model developed by Speziale et al. (1991) (known as SSG model), which was optimized to perform well for a range of benchmark homogeneous shear flows. The coefficients of the SSG model are listed as follows:

$$C_1 = 3.4 + 1.8\left(\frac{P}{\varepsilon}\right), \quad C_2 = 0.36, \quad C_3 = 1.25, \quad C_4 = 0.4 \tag{15}$$

The buoyant part $\phi_{ij,3}$ was modeled by Launder (1996)

$$\phi_{ij,3} = -C_5\left(G_{ij} - \frac{1}{3}G_{kk}\delta_{ij}\right) \tag{16}$$

where C_5 is a constant value of 0.6 as suggested by Launder (1996).

The temperature pressure-gradient correlation is usually modeled in the general form (Wikstrom et al., 2000)

$$\begin{aligned}\phi_{i\theta} = &-C_{\theta 1}\frac{\varepsilon}{K}\overline{u_i\theta} + C_{\theta 2}\overline{u_j\theta}\frac{\partial U_i}{\partial x_j} + C_{\theta 3}\overline{u_j\theta}\frac{\partial U_j}{\partial x_i} \\ &+ C_{\theta 4}\overline{u_i u_j}\frac{\partial T}{\partial x_j} + C_{\theta 5}\beta\overline{\theta^2}g_i\end{aligned} \tag{17}$$

The following constants recommended by Launder (1988) are used:

$$C_{\theta 1} = 3.3, \quad C_{\theta 2} = 0.4, \quad C_{\theta 3} = C_{\theta 4} = 0, \quad C_{\theta 5} = 0.4. \tag{18}$$

2.2.2. Models for ε and ε_θ

At high Reynolds numbers, the viscous dissipation ε_{ij} is usually supposed to be isotropic.

Therefore, the tensor ε_{ij} can be written as: $\varepsilon_{ij} = \frac{2}{3}\varepsilon\delta_{ij}$ where ε, the turbulent dissipation rate of energy, is usually modeled for buoyant flows as follows:

$$\frac{\mathrm{d}\varepsilon}{\mathrm{d}t} = C_{\varepsilon 1}\frac{\varepsilon}{K}(P + C_{\varepsilon 3}G) - C_{\varepsilon 2}\frac{\varepsilon^2}{K} + R_\varepsilon \tag{19}$$

For the standard dissipation equation

$$C_{\varepsilon 1} = 1.44, \quad C_{\varepsilon 2} = 1.83, \quad C_{\varepsilon 3} = 1, \quad R_\varepsilon = 0. \tag{20}$$

whereas for the RNG model of Yakhot et al. (1992):

$$\begin{aligned}&C_{\varepsilon 1} = 1.44, \quad C_{\varepsilon 2} = 1.83, \quad C_{\varepsilon 3} = 1, \\ &R_\varepsilon = -\frac{C_\mu\eta^3(1-\eta/\eta_0)}{1+\beta\eta^3}\left(\frac{\varepsilon^2}{K}\right) \\ &\beta = 0.1, \quad \eta_0 = 5.8, \quad C_\mu = 0.085 \quad \eta = \sqrt{2S_{ij}S_{ij}}\frac{K}{\varepsilon}\end{aligned} \tag{21}$$

The original values of η_0 and β were modified in order to match the DNS data for incompressible homogeneous shear flows.

Zhao et al. (2001) proposed an additional term derived from the anisotropic dissipation tensor model of Speziale and Gatski (1997)

$$\begin{aligned}&C_{\varepsilon 1} = 1.44, \quad C_{\varepsilon 2} = 1.83, \quad C_{\varepsilon 3} = 1, \quad C_{\varepsilon 4} = 0.042, \\ &R_\varepsilon = C_{\varepsilon 4}\varepsilon\sqrt{2S_{ij}S_{ij}}\end{aligned} \tag{22}$$

The value of $C_{\varepsilon 4}$ is too high, and was modified to $C_{\varepsilon 4} = 0.0025$ in order to yield good agreement with the DNS data for the unstratified homogeneous shear flow.

Finally, the Jones and Musonge (1988) (hereafter referred as JM model) model for the viscous dissipation rate of temperature variance ε_θ is considered:

$$\frac{\mathrm{d}\varepsilon_\theta}{\mathrm{d}t} = -C_{d1}\frac{\varepsilon_\theta^2}{\overline{\theta^2}} - C_{d2}\frac{\varepsilon\varepsilon_\theta}{K} + C_{d3}\frac{P_\theta}{\overline{\theta^2}}\varepsilon_\theta + C_{d4}\frac{P}{K}\varepsilon_\theta + C_{d5}\frac{\varepsilon}{K}P_\theta \tag{23}$$

with closure coefficients are given by

$$\begin{aligned}&C_{d1} = 2, \quad C_{d2} = C_{\varepsilon 2} - 1, \quad C_{d3} = 0, \quad C_{d4} = C_{\varepsilon 1}, \\ &C_{d5} = 1.6\end{aligned} \tag{24}$$

The viscous dissipation rate of temperature variance may be obtained from an equilibrium assumption which

assumes that the ratio r between the thermal time scale $\overline{\theta^2}/\varepsilon_\theta$ and the mechanical time scale K/ε is constant but flow dependent.

$$\varepsilon_\theta = \frac{\overline{\theta^2}}{r}\frac{\varepsilon}{K} \tag{25}$$

2.2.3. Turbulence models to be tested

In this paper, three second-order closure models will be tested for the problem of homogeneous stably stratified shear flow. All second-order closure models use the SSG model for the pressure–strain correlation (Eq. (13)), Launder's model for the buoyancy contribution (Eq. (16)) and the JM model for the pressure–temperature gradient (Eq. (17)) and the temperature variance dissipation rate (Eq. (23)) but different dissipation rate equations.

For the sake of clarity, the following abbreviations are adopted to designate the turbulence models to be tested. The model **A** uses the standard dissipation rate equation (Eq. (20)), the model **B** uses the RNG dissipation rate equation (Eq. (21)) and the model **C** uses the dissipation equation of Zhao et al. (2001) (Eq. (22)).

The coefficients η_0, β and $C_{\varepsilon 4}$ in the modeled dissipation rate equations have been calibrated to perform well in incompressible homogeneous shear flows.

2.3. Second-order non-dimensional equations

The second-order closure equations can be non-dimensionalized and recast into an equivalent of equations for the Reynolds stress anisotropy tensor b_{ij}, the parameter (ε/SK), the parameter $(\varepsilon_\theta/S\overline{\theta^2})$, the normalized temperature variance F_θ and the normalized heat flux F_i defined as

$$F_i = \frac{g\beta}{KS}\overline{u_i\theta}, \quad F_\theta = \left(\frac{g\beta}{S}\right)^2\frac{\overline{\theta^2}}{K} \tag{26}$$

The scaling used for the heat flux vector is somewhat non-standard. The usual scaling is through the square root of the product of the turbulent kinetic energy and the temperature variance for the heat flux vector. However, the two scaling coincide because the ratio of the kinetic energy and temperature variance is constant for the flow considered.

The following non-dimensional system of the second-order equations is obtained:

$$\frac{\mathrm{d}K^*}{\mathrm{d}t^*} = -\left(2b_{13} + \frac{\varepsilon}{SK} - F_3\right)K^* \tag{27}$$

$$\begin{aligned}\frac{\mathrm{d}(b_{ij})}{\mathrm{d}t^*} = &-\left(\frac{C_1}{2} - 1 + \left(\frac{P+G}{\varepsilon}\right)\right)\left(\frac{\varepsilon}{Sk}\right)b_{ij} \\ &+ \left(\frac{C_3-2}{2}\right)\left(b_{ik}S^*_{jk} + b_{jk}S^*_{ik} - \frac{2}{3}b_{mn}S^*_{mn}\delta_{ij}\right) \\ &+ \left(\frac{C_4-2}{2}\right)\left(b_{ik}W^*_{jk} + b_{jk}W^*_{ik}\right) + \left(\frac{C_2}{2} - \frac{2}{3}\right)S^*_{ij} \\ &- \left(\frac{C_5-1}{2}\right)\left(F_i\delta_{j3} + F_j\delta_{i3} - \frac{2}{3}F_k\delta_{k3}\delta_{ij}\right)\end{aligned} \tag{28}$$

$$\begin{aligned}\frac{\mathrm{d}}{\mathrm{d}t^*}\left(\frac{\varepsilon}{SK}\right) = &\left[(C_{\varepsilon 1}-1)\left(\left(\frac{P}{\varepsilon}\right) + \left(\frac{C_{\varepsilon 1}C_{\varepsilon 3}-1}{C_{\varepsilon 1}-1}\right)\left(\frac{G}{\varepsilon}\right)\right)\right. \\ &\left. + (1-C_{\varepsilon 2}) + R^*_\varepsilon\right]\left(\frac{\varepsilon}{SK}\right)^2\end{aligned} \tag{29}$$

$$\begin{aligned}\frac{\mathrm{d}F_i}{\mathrm{d}t^*} = &-2(1-C_{\theta 4})\left(b_{ik} + \frac{\delta_{ik}}{3}\right)Ri\delta_{k3} - (C_{\theta 5}-1)F_\theta\delta_{i3} \\ &+ (C_{\theta 2}-1)F_k\delta_{k3}\delta_{i1} + C_{\theta 3}F_k\delta_{k1}\delta_{i3} \\ &- \left(C_{\theta 1} - 1 + \left(\frac{P+G}{\varepsilon}\right)\right)\left(\frac{\varepsilon}{SK}\right)F_i\end{aligned} \tag{30}$$

$$\frac{\mathrm{d}F_\theta}{\mathrm{d}t^*} = -2RiF_k\delta_{k3} - \left(\left(\frac{P+G}{\varepsilon}\right) - 1 + \frac{2}{r}\right)\left(\frac{\varepsilon}{SK}\right)F_\theta \tag{31}$$

$$\begin{aligned}\frac{\mathrm{d}}{\mathrm{d}t^*}\left(\frac{\varepsilon_\theta}{S\overline{\theta^2}}\right) = &\left((2-C_{d1}) - (2-C_{d3}-rC_{d5})\left(\frac{P_\theta}{\varepsilon_\theta}\right)\right. \\ &\left. - r\left(C_{d2} - C_{d4}\left(\frac{P}{\varepsilon}\right)\right)\right)\left(\frac{\varepsilon_\theta}{S\overline{\theta^2}}\right)^2\end{aligned} \tag{32}$$

where $Ri = g\beta S_T/S^2$ is the gradient Richardson number and $r = (\varepsilon/SK)/\left(\varepsilon_\theta/S\overline{\theta^2}\right)$. The non-dimensional quantities are

$$t^* = St, \quad K^* = \frac{K}{K_0}, \quad S^*_{ij} = \frac{S_{ij}}{S}, \quad W^*_{ij} = \frac{W_{ij}}{S}, \quad R^*_\varepsilon = \frac{R_\varepsilon}{\varepsilon S}\left(\frac{SK}{\varepsilon}\right) \tag{33}$$

Note that $(P/\varepsilon) = -2b_{13}(SK/\varepsilon)$ and $(G/\varepsilon) = F_3(SK/\varepsilon)$.

The above system of non-linear ordinary differential equations associated with each turbulence model is solved subjected to the initial conditions:

$$\left(\frac{\varepsilon}{SK}\right) = \left(\frac{\varepsilon_0}{SK_0}\right); \quad b_{ij} = 0; \quad F_i = 0; \quad F_\theta = 0; \quad \left(\frac{\varepsilon_0}{SK_0}\right) = \frac{1}{r}\left(\frac{\varepsilon_0}{SK_0}\right)$$

at time $t^* = 0$, which correspond to a state of isotropic turbulence.

Equilibrium states of turbulence are determined by setting the time derivatives on the left-hand sides of equations to zero. The resulting non-linear system of algebraic equations leads to a set of equilibrium values $((b_{11})_\infty, (b_{22})_\infty, (b_{33})_\infty, (b_{13})_\infty, (\varepsilon/SK)_\infty, (\varepsilon_\theta/S\overline{\theta^2})_\infty, (F_3)_\infty, (F_1)_\infty, (F_\theta)_\infty)$, provided that the equilibrium state exists. The equilibrium values, which depend on a single parameter the gradient Richardson number Ri, are denoted by subscript ∞.

3. Discussion of results

The transport Eqs. (27)–(32) with the models discussed in Section 2 incorporated, were solved numerically for stratified homogeneous shear flow using a fourth-order accurate Runge–kutta numerical integration scheme. Due to isotropic initial conditions, the solution depends on the gradient Richardson number Ri and the initial condition of $SK_0/\varepsilon_0 = 2$.

Experimental and direct numerical simulation data of stratified homogeneous shear flows will be used to evaluate the turbulence models.

3.1. Analysis of modeled dissipation rate equations

In this subsection, an analysis of the consistency of three modeled dissipation rate equations with the existence of stationary states is conducted.

First, we consider the standard dissipation equation (Eqs. (19) and (20)). The equilibrium value of (ε/SK) is determined by setting the time derivative of (ε/SK) to zero in (29) which yields

$$\left(\frac{P}{\varepsilon}\right)_\infty + \left(\frac{C_{\varepsilon1}C_{\varepsilon3}-1}{C_{\varepsilon1}-1}\right)\left(\frac{G}{\varepsilon}\right)_\infty = \frac{C_{\varepsilon2}-1}{C_{\varepsilon1}-1} \tag{34}$$

It follows that

$$\begin{aligned} E_\infty &= \left(\frac{P}{\varepsilon}\right)_\infty + \left(\frac{G}{\varepsilon}\right)_\infty \\ &= \left(\frac{C_{\varepsilon2}-1}{C_{\varepsilon1}-1}\right) + \left(\frac{C_{\varepsilon1}(C_{\varepsilon3}-1)}{C_{\varepsilon1}-1}\right)\left(\frac{-G}{\varepsilon}\right)_\infty \end{aligned} \tag{35}$$

The dimensionless equilibrium growth rate of K (i.e., when $t^* \gg 1$) defined by

$$\gamma_\infty = \left(\frac{1}{K^*}\frac{\mathrm{d}K^*}{\mathrm{d}t^*}\right)_\infty = -\left(2(b_{13})_\infty + \left(\frac{\varepsilon}{SK}\right)_\infty - (F_3)_\infty\right) \tag{36}$$

is related to the parameter E_∞ by

$$\begin{aligned} \gamma_\infty &= (E_\infty - 1)\left(\frac{\varepsilon}{SK}\right)_\infty \\ &= \left(\frac{C_{\varepsilon2}-C_{\varepsilon1}}{C_{\varepsilon1}-1}\right) + \left(\frac{C_{\varepsilon1}(C_{\varepsilon3}-1)}{C_{\varepsilon1}-1}\right)\left(\frac{-G}{\varepsilon}\right)_\infty \end{aligned} \tag{37}$$

If the model constant $C_{\varepsilon3}$ is taken as one, a value usually used by turbulence models, then we have:

$$E_\infty = \left(\frac{P+G}{\varepsilon}\right)_\infty = \frac{C_{\varepsilon2}-1}{C_{\varepsilon1}-1} = \text{const} \tag{38}$$

$$\gamma_\infty = \left(\frac{C_{\varepsilon2}-C_{\varepsilon1}}{C_{\varepsilon1}-1}\right)\left(\frac{\varepsilon}{SK}\right)_\infty \tag{39}$$

The above relation shows that the equilibrium growth rate γ_∞ is always positive which implies that the turbulent kinetic energy increases exponentially. This feature is not supported by experimental and DNS findings: existence of a stationary state ($\gamma_\infty = 0$) at a certain value of the gradient Richardson number $Ri = Rs$ (hereafter referred to as the stationary gradient Richardson number), exponential growth of K ($\gamma_\infty > 0$) for $Ri < Rs$ and exponential decay of K ($\gamma_\infty < 0$) for $Ri > Rs$. Note that the statistical turbulent quantities (such as the turbulent kinetic and the dissipation rate) stay constant in time at $Ri = Rs$.

On the other hand, the standard dissipation equation predicts a $E_\infty = \text{const}$, where the constant is model dependent but independent of the gradient Richardson number, a fact which is not consistent with observation. These deficiencies are due to the inability of the model to predict the existence of the stationary gradient Richardson number.

In fact, the stationary conditions for K and ε $\left(\frac{\mathrm{d}K}{\mathrm{d}t} = \frac{\mathrm{d}\varepsilon}{\mathrm{d}t} = 0\right)$ are:

$$P + G = \varepsilon \tag{40}$$

$$(P + C_{\varepsilon3}G)G = \frac{C_{\varepsilon2}}{C_{\varepsilon1}}\varepsilon \tag{41}$$

The combination of relations (40) and (41) leads to

$$(C_{\varepsilon3}-1)\left(\frac{G}{\varepsilon}\right) = \frac{C_{\varepsilon2}-C_{\varepsilon1}}{C_{\varepsilon1}} \tag{42}$$

The above equation shows that the stationary conditions are not satisfied for $C_{\varepsilon3} = 1$. Therefore, the standard dissipation equation cannot predict the existence of a stationary state for the coefficient $C_{\varepsilon3} = 1$.

The constraint (42) is satisfied for $C_{\varepsilon3} < 1$ given that $((G/\varepsilon) < 0$ and $(C_{\varepsilon2} > C_{\varepsilon1}))$.

If we take $C_{\varepsilon3} < 1$, Eq. (35) shows that the parameter E_∞ decreases with increasing Ri. Also, the dimensionless equilibrium growth rate γ_∞ can be positive, zero or negative (see Eq. (37)). Hence, the standard dissipation equation can predict the existence of a stationary gradient Richardson number, Rs, below which, the turbulent kinetic energy, K, shows exponential growth ($\gamma_\infty > 0$) and, above which, K decays exponentially ($\gamma_\infty < 0$). Of course, the stationary gradient Richardson number Rs will have a non-linear dependence on the model coefficient $C_{\varepsilon3}$ ($Rs = Rs(C_{\varepsilon3})$).

Second we consider the dissipation rate equation of Zhao et al. (2001) (Eqs. (19) and (22)). The stationary conditions of K and ε simplify to

$$P + G = \varepsilon \tag{43}$$

$$(P + C_{\varepsilon3}G) = \frac{C_{\varepsilon2}}{C_{\varepsilon1}}\varepsilon - \left(\frac{C_{\varepsilon4}}{C_{\varepsilon1}}\right)(SK) \tag{44}$$

Combining Eqs. (43) and (44) yields

$$(C_{\varepsilon3}-1)\left(\frac{G}{\varepsilon}\right) = \left(\frac{C_{\varepsilon2}-C_{\varepsilon1}}{C_{\varepsilon1}}\right) - C_{\varepsilon4}\left(\frac{SK}{\varepsilon}\right) \tag{45}$$

For $C_{\varepsilon3} = 1$, the constraint (45) is satisfied when $(SK/\varepsilon)_\infty = (C_{\varepsilon2} - C_{\varepsilon1})/C_{\varepsilon4} \approx 160$, a result not consistent with recent findings of Shih et al. (2000), which indicate that $(SK/\varepsilon)_\infty = 5.5$ at $Ri = Rs$.

Equilibrium values of (ε/SK), E and γ are given by:

$$\begin{aligned} &(C_{\varepsilon1}-1)\left(\frac{P}{\varepsilon}\right)_\infty + (C_{\varepsilon1}C_{\varepsilon3}-1)\left(\frac{G}{\varepsilon}\right)_\infty + (1-C_{\varepsilon2}) \\ &\quad + C_{\varepsilon4}\left(\frac{SK}{\varepsilon}\right)_\infty = 0 \end{aligned} \tag{46}$$

$$\begin{aligned} E_\infty = &\left(\frac{C_{\varepsilon2}-1}{C_{\varepsilon1}-1}\right) + \left(\frac{C_{\varepsilon1}(C_{\varepsilon3}-1)}{C_{\varepsilon1}-1}\right)\left(\frac{-G}{\varepsilon}\right)_\infty \\ &- \left(\frac{C_{\varepsilon4}}{C_{\varepsilon1}-1}\right)\left(\frac{SK}{\varepsilon}\right)_\infty \end{aligned} \tag{47}$$

$$\gamma_\infty = \left(\frac{C_{\varepsilon 2} - C_{\varepsilon 1}}{C_{\varepsilon 1} - 1}\right) + \left(\frac{C_{\varepsilon 1}(C_{\varepsilon 3} - 1)}{C_{\varepsilon 1} - 1}\right)\left(\frac{-G}{\varepsilon}\right)_\infty - \left(\frac{C_{\varepsilon 4}}{C_{\varepsilon 1} - 1}\right)\left(\frac{SK}{\varepsilon}\right)_\infty \quad (48)$$

When $C_{\varepsilon 3} < 1$, the parameter E_∞ decreases as Ri increases given that $C_{\varepsilon 2} > C_{\varepsilon 1}$ and $C_{\varepsilon 1} > 1$. Also the dimensionless equilibrium growth γ_∞ can be positive, zero or negative. It is thus clear that the model can properly describe the basic physics of homogeneous stratified flows provided that $C_{\varepsilon 3} < 1$.

Third, we consider the RNG dissipation rate equation (Eqs. (19) and (21)). The additional extra-term in the RNG dissipation equation can increase or decrease the source of the dissipation depending whether the parameter $\eta = (SK/\varepsilon)$ is larger or smaller, respectively to the equilibrium value for homogeneous shear flow ($\eta_0 = 5.8$).

The use of the stationary conditions of K and ε leads to

$$(C_{\varepsilon 3} - 1)\left(\frac{G}{\varepsilon}\right) = \left(\frac{C_{\varepsilon 2} - C_{\varepsilon 1}}{C_{\varepsilon 1}}\right) + \frac{C_\mu}{C_{\varepsilon 1}}\frac{\eta^3(1 - \eta/\eta_0)}{1 + \beta\eta^3} \quad (49)$$

The constraint (49) is satisfied for $(SK/\varepsilon)_\infty = 8.5$ for given coefficient $C_{\varepsilon 1}$, $C_{\varepsilon 2}$, β and C_μ, which is not in the experimental range of 5–6.

Equilibrium values of (ε/SK), E and γ are given by:

$$(C_{\varepsilon 1} - 1)\left(\frac{P}{\varepsilon}\right)_\infty + (C_{\varepsilon 1}C_{\varepsilon 3} - 1)\left(\frac{G}{\varepsilon}\right)_\infty + (1 - C_{\varepsilon 2}) - \frac{C_\mu\eta^3(1 - \eta/\eta_0)}{1 + \beta\eta^3} = 0 \quad (50)$$

$$E_\infty = \left(\frac{C_{\varepsilon 2} - 1}{C_{\varepsilon 1} - 1}\right) + \left(\frac{C_{\varepsilon 1}(C_{\varepsilon 3} - 1)}{C_{\varepsilon 1} - 1}\right)\left(\frac{-G}{\varepsilon}\right)_\infty + \frac{C_\mu\eta^3(1 - \eta/\eta_0)}{(1 + \beta\eta^3)(C_{\varepsilon 1} - 1)} \quad (51)$$

$$\gamma_\infty = \left(\frac{C_{\varepsilon 2} - C_{\varepsilon 1}}{C_{\varepsilon 1} - 1}\right) + \left(\frac{C_{\varepsilon 1}(C_{\varepsilon 3} - 1)}{C_{\varepsilon 1} - 1}\right)\left(\frac{-G}{\varepsilon}\right)_\infty + \frac{C_\mu\eta^3(1 - \eta/\eta_0)}{(1 + \beta\eta^3)(C_{\varepsilon 1} - 1)} \quad (52)$$

For $C_{\varepsilon 3} < 1$, The above equations show that the basic features of homogeneous stratified flows can be reproduced.

In conclusion, the above analysis shows that the modeled standard dissipation equation (with $C_{\varepsilon 3} = 1$), is highly deficient in that it cannot predict the essential features of homogeneous stratified flows, i.e., exponential growth and exponential decay of K. The introduction of extra-term in the standard equation, which is developed to take into account non-equilibrium effects and dissipation anisotropy, do not improve significantly the prediction. However, if we take $C_{\varepsilon 3} < 1$, a sufficient condition for the existence of a stationary state, the basic features of the homogeneous sheared stratified flow are reproduced.

3.2. Discussion of the results

In this section, model predictions are presented for the test problem of stratified homogeneous shear flow. Comparisons are made with experimental and numerical simulation data.

First, we investigate the sensitivity of the prediction of stationary states to the model coefficient $C_{\varepsilon 3}$.

Fig. 1 shows the variation of the predicted stationary gradient number Rs as a function of the model coefficient $C_{\varepsilon 3}$, for various turbulence models. In accordance with the findings of the previous analysis, a stationary state is predicted for the range of values reported in the literature, $0.14 < Rs < 0.25$, when the coefficient $C_{\varepsilon 3} < 1$. Also, it can be seen that the coefficient $C_{\varepsilon 3}$ monotonically increases with Rs. Evidently, as the coefficient $C_{\varepsilon 3}$ decreases, the parameter $(-G/\varepsilon)$ decreases (see Eqs. (42), (45) and (49)), which, in turn, decreases R_f and Rs. Essentially, the coefficient $C_{\varepsilon 3}$, by controlling the level of dissipation due to buoyancy in the dissipation rate equation, improves the capability of models to predict stationary states.

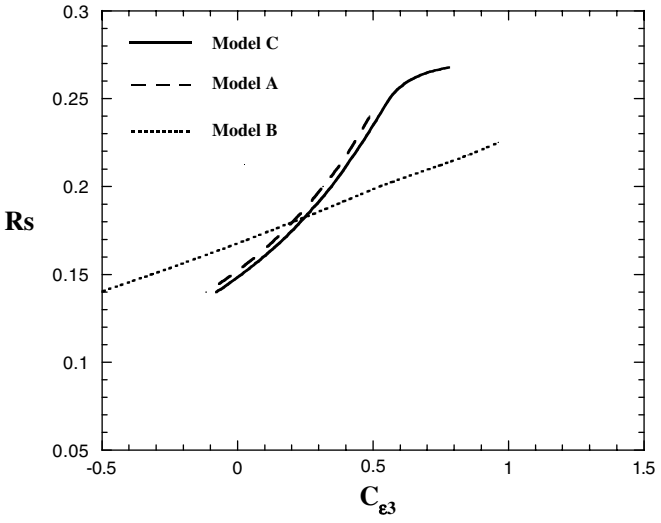

Fig. 1. Variation of Rs with $C_{\varepsilon 3}$ for different models.

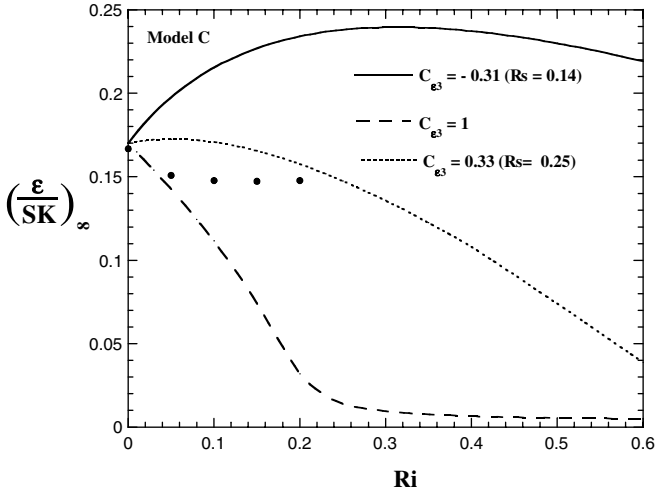

Fig. 2. Equilibrium diagram of (ε/SK) for the model **C** using different values of $C_{\varepsilon 3}$. Direct numerical simulations of Jacobitz et al. (1997) are shown (symbols).

Second, the effect of the model coefficient $C_{\varepsilon 3}$ on the performance of the model **C** is assessed. In Fig. 2, equilibrium diagrams of (ε/SK) are shown as a function of Ri, for the model **C** using three different values of $C_{\varepsilon 3}$ ($C_{\varepsilon 3} = 1$, $C_{\varepsilon 3} = -0.31$ and $C_{\varepsilon 3} = 0.33$) corresponding respectively to $Rs = 0.14$ and $Rs = 0.25$. Some conclusions can be drawn from these results: (a) second-order closure models are capable of accounting the stabilizing effects of stable stratification in turbulent shear flow, i.e., decrease of the parameter $(\varepsilon/SK)_\infty$ as Ri increases, (b) when the $C_{\varepsilon 3} = 1$, the model **C** drastically underpredicts the parameter $(\varepsilon/SK)_\infty$, while the model predictions with $C_{\varepsilon 3} < 1$, compares more favourably with DNS data, (c) the range of flow destabilization ($0 < Ri < Rc$) is lengthened as the coefficient $C_{\varepsilon 3}$ decreases (note that turbulence collapses at $Ri = Rc$, which is of order one).

Furthermore, the basic model **C** (with $C_{\varepsilon 3} = 1$) erroneously predicts a universal equilibrium value of the ratio production to dissipation E_∞, independent of Ri in the range of flow destabilisation (see Fig. 3). Consequently, as shown in Fig. 4, an exponential growth of K is erroneously predicted for $0 < Ri < Rc$ (the equilibrium growth rate $\gamma_\infty > 0$).

It is thus clear that the reason for these poor predictions is due to the failure of the basic model to predict the existence of a stationary state.

In contrast, the model **C** with $C_{\varepsilon 3} < 1$, yields substantially better results than the basic model. The stabilizing effect of stratification on turbulent shear flow is captured: exponential growth of K ($\gamma_\infty > 0$) for $Ri < Rs$, exponential decay of K ($\gamma_\infty < 0$) for $Rs < Ri < Rc$, stationary state at $Ri = Rs$ (see Fig. 4). It follows that the model **C** yields equilibrium values of E (see Fig. 3), which compare favourably to the DNS data. This is not surprising result because equilibrium values of turbulent quantities are tied to the equilibrium growth rate γ_∞ (Eqs. (35) and (36)).

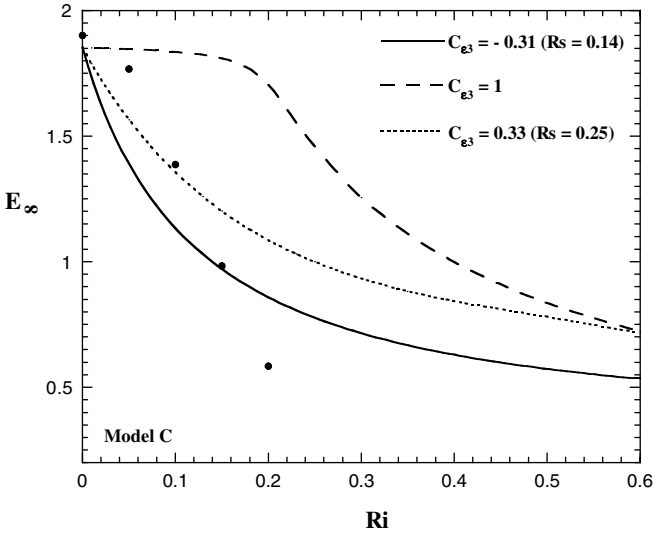

Fig. 3. Equilibrium diagram of E for the model **C** using different values of $C_{\varepsilon 3}$. Direct numerical simulations of Jacobitz et al. (1997) are shown (symbols).

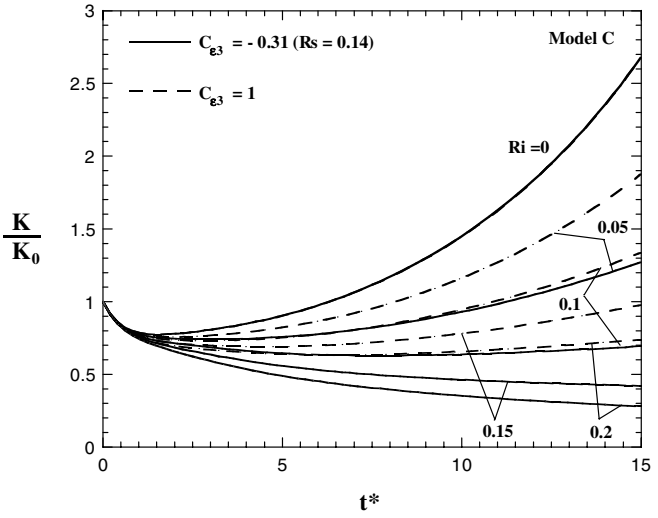

Fig. 4. Time evolution of the turbulent kinetic energy K using $\varepsilon_0/SK_0 = 0.5$, for the model **C** with different values of Ri.

Attention is now turned to the comparisons between the model **C** predictions of equilibrium states with the high Re homogeneous shear flow of Webster (1964) who attempted to produce such flow in a heated wind tunnel. However, his turbulence correlation show a dependence on the streamwise direction. In spite of these deficiencies, we used his data at his most downstream station in the study.

The turbulent Prandtl number P_{rt} is defined as the ratio between eddy viscosity ν_t and eddy diffusivity α_t, or, equivalently, the ratio between the gradient Richardson number Ri and the flux Richardson number. Fig. 5 shows the variation of the predicted P_{rt} normalised by its neutral value ($P_{rt_0} = 0.6$) as a function of Ri. The model **C** (with $C_{\varepsilon 3} = -0.31$), reproduces the observed dependence of P_{rt} on stratification despite the considerable scatter in the

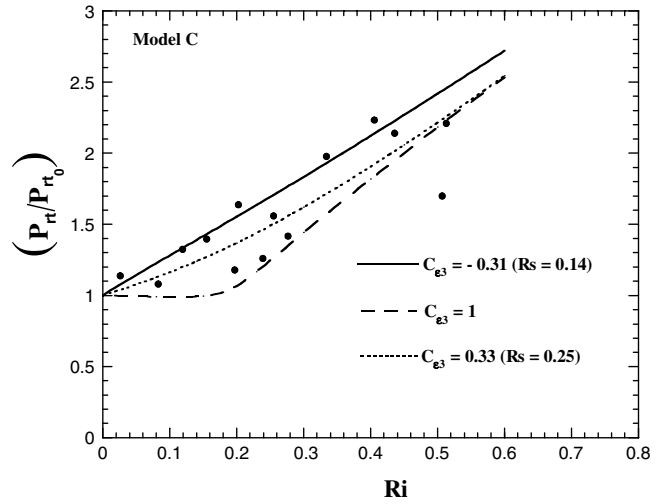

Fig. 5. Equilibrium diagram of (P_{rt}/P_{rt_0}) for the model **C** using different values of $C_{\varepsilon 3}$. Experimental data of Webster (1964) are shown (symbols).

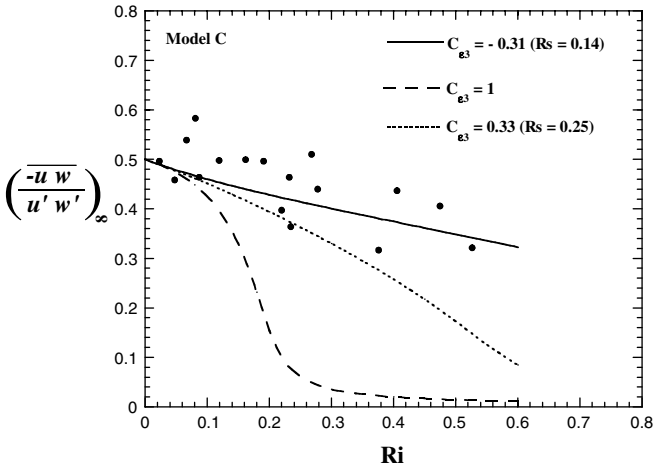

Fig. 6. Equilibrium diagram of $(\overline{uw}/u'w')$ for the model **C** using different values of $C_{\varepsilon 3}$. Experimental data of Webster (1964) are shown (symbols).

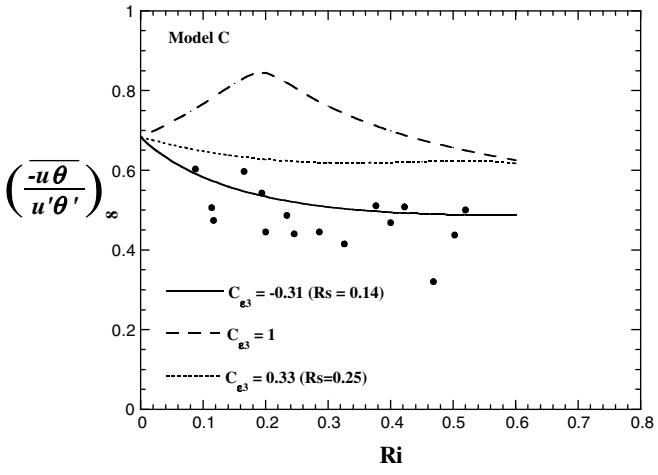

Fig. 8. Equilibrium diagram of $(\overline{u\theta}/u'\theta')$ for the model **C** using different values of $C_{\varepsilon 3}$. Experimental data of Webster (1964) are shown (symbols).

measured data. The predicted equilibrium shear stress correlation coefficient $(\overline{uw}/u'w')$ is shown in Fig. 6. The model **C** (with $C_{\varepsilon 3} = -0.31$) correctly predicts the behaviour of this coefficient with Ri: slow decrease for $Ri < 0.25$ and then rapid decrease for $Ri > 0.25$.

As Ri increases, the predicted vertical heat flux correlation dramatically decreases while the horizontal heat flux correlation coefficient slightly decreases, in agreement with experimental results (see Figs. 7 and 8).

Third, the effect of the coefficient $C_{\varepsilon 3}$ on the prediction of the length scales is assessed. Among the relevant length scales used to characterize the state of turbulence in a stratified flow, are the Ozmidov scale L_O, the Ellison scale L_E and the buoyancy length scale L_b.

The Ozmidov scale $L_O = (\varepsilon/N^3)^{1/2}$ represents the scale of motion at which buoyancy forces become of the same order of magnitude as inertial forces. Therefore, the scale L_O gives an upper bound for the size of turbulent density overturns. Scales larger than L_O are dominated by buoyancy and cannot overturn. The buoyancy length scale $L_b = (\overline{w^2})^{1/2}/N$ is defined as the vertical distance travelled by a fluid particle in converting kinetic energy into potential energy. Therefore, L_b sets un upper limit for the largest vertical scale of turbulence in a stratified flow. The Ellison scale $L_E = (\overline{\theta^2})^{1/2}/S_T$ represents the vertical distance a fluid particle travels before either returning to its equilibrium level or mixing. The scale L_E can be computed with the second-order closure model.

Figs. 9 and 10 show the time evolution of the predicted normalized length scales L_O, L_b and L_E for the model **C** with $Ri = 0.1$ and $Ri = 0.2$.

For $Ri = 0.1$, as the flow evolves, the predicted kinetic energy increases exponentially and the predicted length scales L_O, L_b and L_E increase with time. However, the growth of the scales is much faster when $C_{\varepsilon 3} = 1$.

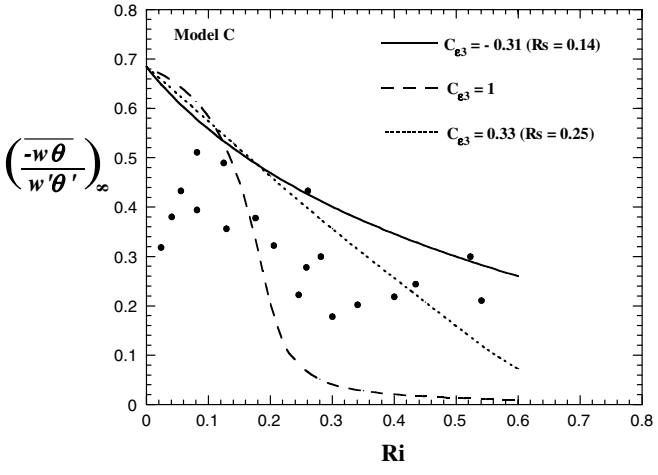

Fig. 7. Equilibrium diagram of $(\overline{w\theta}/w'\theta')$ for the model **C** using different values of $C_{\varepsilon 3}$. Experimental data of Webster (1964) are shown (symbols).

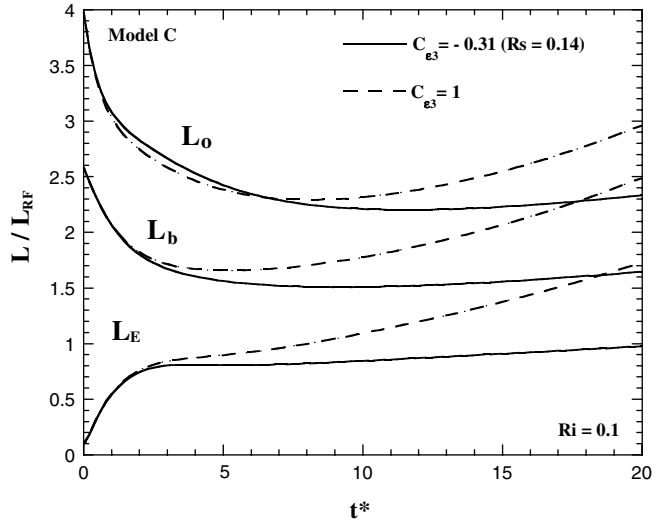

Fig. 9. Time evolution of length scales L_O, L_b and L_E for the model **C** at $Ri = 0.1$.

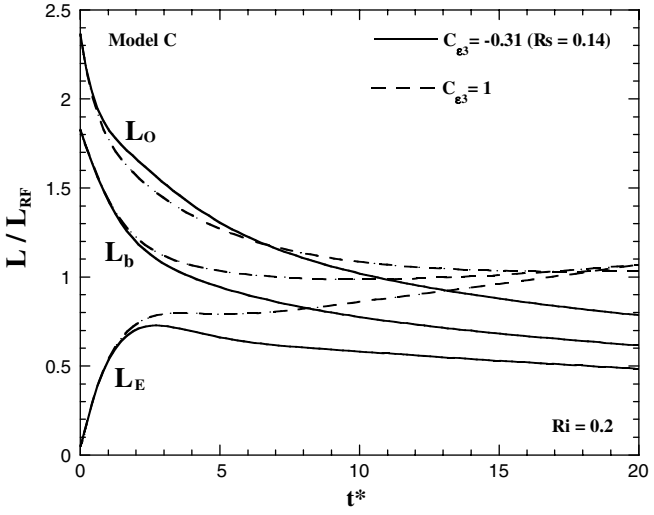

Fig. 10. Time evolution of length scales L_O, L_b and L_E for the model **C** at $Ri = 0.2$.

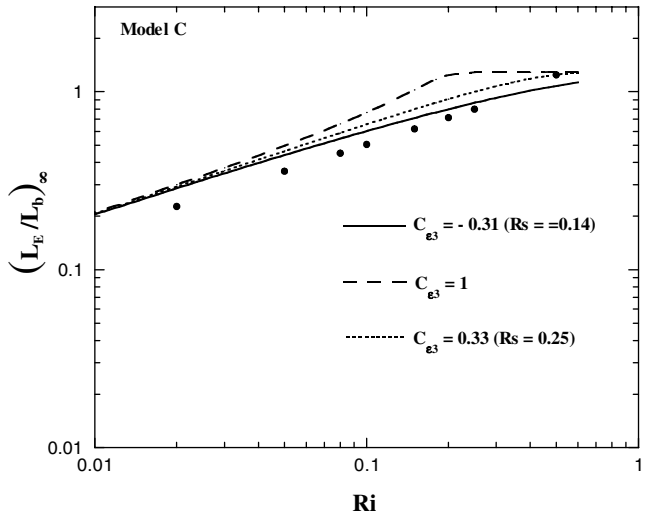

Fig. 12. Equilibrium diagram of (L_E/L_b) for the model **C** using different values of $C_{\varepsilon 3}$. Experimental data of Rohr et al. (1988) are shown (symbols).

For $Ri = 0.2 > Rs = 0.14$, the turbulence model **C** with $C_{\varepsilon 3} = -0.31$, which predicts an exponential decay of K, predicts the decrease of length scales L_O, L_b and L_E with time as buoyancy suppresses the turbulent eddies.

This result is consistent with the experimental and numerical simulation findings (Rohr et al., 1988; Jacobitz, 2002). As the buoyancy scale increases, the Ozmidov scale L_O decreases which restricts the evolution of the Ellison length scale L_E. Therefore, the vertical overturn is restricted and decay of the turbulent kinetic energy results. However, the basic model (with $C_{\varepsilon 3} = 1$), which predicts an exponential growth of K, predicts an erroneous increase of the length scales as time advances.

In Figs. 11 and 12, the predicted equilibrium values of (L_E/L_O) and (L_E/L_b) are compared to the following empirical curves (Rohr et al., 1988):

$$L_E/L_O = 4.2(Ri)^{3/4} \quad L_E/L_b = 1.6(Ri)^{1/2}$$

It can be seen that the turbulence model **C** with $C_{\varepsilon 3} < 1$, yields better predictions than the basic model for moderate stratified homogeneous flows ($Ri < 0.2$).

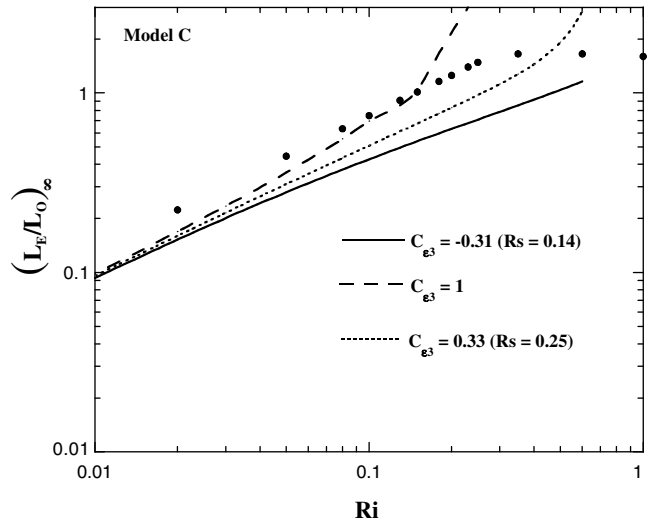

Fig. 11. Equilibrium diagram of (L_E/L_O) for the model **C** using different values of $C_{\varepsilon 3}$. Experimental data of Rohr et al. (1988) are shown (symbols).

4. Conclusions

An assessment of second-order closure models in the prediction of stably stratified homogeneous shear flows has been conducted. The emphasis is focused on the effect of modelled dissipation rate equation on the predictions of these flows. It has been demonstrated that the performance of the models considered was found to be quite poor.

The main features of the flow considered, i.e., the existence of stationary gradient Richardson number, Rs, exponential growth of K ($Ri < Rs$) and exponential decay of K ($Ri > Rs$) are not reproduced by all models. The origin of the deficient predictions appears to be tied to the modeling of the dissipation rate equation, which does not satisfy the stationary conditions.

In fact, if the model coefficient $C_{\varepsilon 3}$ in the dissipation equation is taken less than one, a sufficient condition for the existence of a stationary state, all second-order closure models reproduce the basic features of the homogeneous sheared stratified flows.

Note that the value of the model coefficient $C_{\varepsilon 3}$ should be determined using high Reynolds equilibrium flows.

References

Abid, R., Speziale, C.G., 1993. Predicting equilibrium states with Reynolds stress closure in channel flow and homogeneous shear flow. Phys. Fluids A 5, 1776.

Craft, T.J., Launder, B.E., 2001. Principles and performance of TCL-based second-moment closure. Flow Turbul. Combust. 66, 355.

Craft, T.J., Ince, N.Z., Launder, B.E., 1996. Recent developments in second-moment closure for buoyancy affected flows. Dynam. Atmos. Oceans 23, 99.

Gerz, T., Schumann, U., Elghobashi, S.E., 1989. Direct numerical simulation of stratified homogeneous turbulent shear flows. J. Fluid Mech. 200, 563.

Holt, S.E., Koseff, J.R., Ferziger, J.H., 1992. A numerical study of the evolution and structure of homogeneous turbulent shear flows. J. Fluid Mech. 237, 499.

Jacobitz, F.G., 2000. Scalar transport and mixing in turbulent stratified shear flow. Int. J. Heat Fluid Flow 21, 535.

Jacobitz, F.G., 2002. A comparison of the turbulence evolution in a stratified fluid with vertical or horizontal shear. J. Turbul. 3, 1.

Jacobitz, F.G., Sarkar, S., 1998. The effect of non vertical shear on turbulence in a stably stratified medium. Phys. Fluids 10, 1185.

Jacobitz, F.G., Sarkar, S., 1999. A direct numerical study of transport and anisotropy in a stably stratified turbulent flow with uniform horizontal shear. Flow Turbul. Combust. 63, 343.

Jacobitz, F.G., Sarkar, S., Van Atta, C.W., 1997. Direct numerical simulation of the turbulence evolution in a uniformly sheared and stably stratified flow. J. Fluid Mech. 342, 231.

Jones, W.P., Musonge, P., 1988. Closure of the Reynolds stress and scalar flux equations. Phys. Fluids 31, 3589.

Kaltenbach, H.J., Gerz, T., Schumann, U., 1994. Large-eddy simulation of homogeneous turbulence and diffusion in stably stratified shear flow. J. Fluid Mech. 280, 1.

Launder, B.E., 1996. An introduction to single-point closure methodology. In: Simulation and modelling of turbulent flows. Oxford University Press, p. 243.

Launder, B.E., 1988. The prediction of forced-field effects, on turbulent shear flow in second-moment closure. In: Fernholtz, H.H., Fieler, H.E. (Eds.), Advances in Turbulence. Springer, p. 338.

Miles, J.W., 1961. On the stability of heterogeneous shear flows. J. Fluid Mech. 10, 496.

Piccirillo, P.S., Van Atta, C.W., 1997. The evolution of a uniformly sheared thermally stratified turbulent flow. J. Fluid Mech. 334, 61.

Rohr, J.J., Itsweire, C., Helland, K.N., Van Atta, W., 1988. Growth and decay of turbulence in a stably stratified shear flow. J. Fluid Mech. 65, 77.

Shih, L.H., Koseff, J.R., Ferziger, J.H.F., Rehmann, C.R., 2000. Scaling and parameterization of stratified homogeneous shear flow. J. Fluid Mech., 412.

Speziale, C.G., Gatski, T.B., 1997. Analysis and modeling of anisotropies in the dissipation rate of turbulence. J. Fluid Mech. 344, 155.

Speziale, C.G., Sarkar, S., Gatski, T.B., 1991. Modeling the pressure strain correlation of turbulence: An invariant dynamical system approach. J. Fluid Mech. 227, 245.

Webster, C.A.G., 1964. An experimental study of turbulence in density stratified shear flow. J. Fluid Mech. 19, 221.

Wikstrom, P.M., Wallin, S., Johanson, A.V., 2000. Derivation and integration of a new explicit algebraic model for the passive scalar flux. Phys. Fluids 12, 688.

Yakhot, V., Orszag, S.A., Thangam, S., Gatski, T.B., Speziale, C.G., 1992. Development of turbulence models for shear flows by a double expansion technique. Phys. Fluids A 4, 1510.

Zhao, C.Y., So, R.MC., Gatski, T.B., 2001. Turbulence modeling effects on the prediction of equilibrium of buoyant shear flow. Theor. Comput. Fluid Dynam. 14, 399.